

pubs.acs.org/est Article

Relating Molecular Properties to the Persistence of Marine Dissolved Organic Matter with Liquid Chromatography-Ultrahigh-Resolution **Mass Spectrometry**

Rene M. Boiteau,* Yuri E. Corilo, William R. Kew, Christian Dewey, Maria Cristina Alvarez Rodriguez, Craig A. Carlson, and Tim M. Conway



Cite This: Environ. Sci. Technol. 2024, 58, 3267-3277



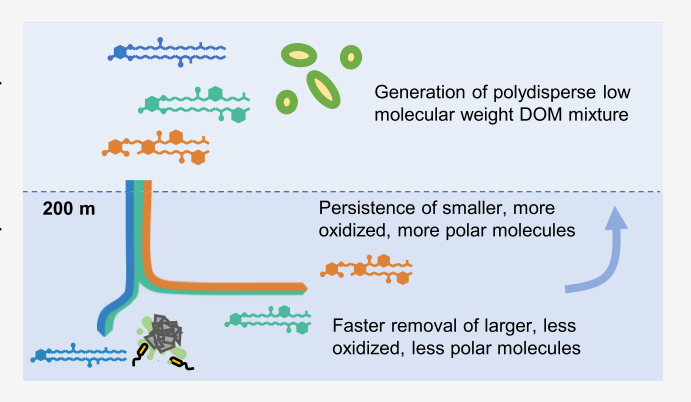
ACCESS I

III Metrics & More

Article Recommendations

Supporting Information

ABSTRACT: Marine dissolved organic matter (DOM) contains a complex mixture of small molecules that eludes rapid biological degradation. Spatial and temporal variations in the abundance of DOM reflect the existence of fractions that are removed from the ocean over different time scales, ranging from seconds to millennia. However, it remains unknown whether the intrinsic chemical properties of these organic components relate to their persistence. Here, we elucidate and compare the molecular compositions of distinct DOM fractions with different lability along a water column in the North Atlantic Gyre. Our analysis utilized ultrahighresolution Fourier transform ion cyclotron resonance mass spectrometry at 21 T coupled to liquid chromatography and a novel data pipeline developed in CoreMS that generates molecular formula assignments and metrics of isomeric complexity.



Clustering analysis binned 14 857 distinct molecular components into groups that correspond to the depth distribution of semilabile, semirefractory, and refractory fractions of DOM. The more labile fractions were concentrated near the ocean surface and contained more aliphatic, hydrophobic, and reduced molecules than the refractory fraction, which occurred uniformly throughout the water column. These findings suggest that processes that selectively remove hydrophobic compounds, such as aggregation and particle sorption, contribute to variable removal rates of marine DOM.

KEYWORDS: Dissolved organic matter, liquid chromatography, high-resolution mass spectrometry, ocean carbon cycle, particle reactivity

INTRODUCTION

The apparent reactivity of marine dissolved organic matter (DOM) is known to vary systematically across both spatial and temporal scales. A "labile" fraction of DOM is generated when biomolecules are released from biological processes, including extracellular photoautotrophic production, viral lysis, particle solubilization, and zooplankton excreta. 1,2 The production of labile DOM is most pronounced in the surface ocean, where it is quickly degraded on rapid time scales (i.e., seconds to weeks), precluding its accumulation to appreciable concentrations.^{3,4} In contrast, the forms of DOM that resist degradation account for most of the marine organic carbon inventory. From the synthesis of ocean-wide dissolved organic carbon (DOC) concentration and radiocarbon measurements, marine DOM has been further classified into semilabile (SLDOM), semirefractory (SRDOM), and refractory (RDOM) fractions with inferred removal time scales of months, decades, or millennia. 5,6 While the persistence of these fractions underpin global distributions of marine organic

carbon and nutrients, their origin and chemical distinctions remain unclear.^{7,8}

The existence of fractions with different removal rates indicates that certain molecular components of DOM are more persistent than others, $^{3,9-11}$ and several explanations have been proposed. DOM persistence may reflect the transformation of DOM into molecules that are so highly diversified that each is at its limiting concentration of metabolic utility. 12-15 Another explanation is that the intrinsic properties of DOM determine persistence. For example, chemical composition may make certain molecules more resistant to degradation (recalcitrant). 16 Some components of DOM could be preferentially incorporated into aggregates or sorb to particles that are

October 5, 2023 Received: Revised: November 28, 2023 Accepted: January 18, 2024 Published: February 9, 2024





hotspots of biodegradation and can settle out of the water column. ^{17,18} Biodegradation experiments have demonstrated that larger class sizes of organic matter are more rapidly remineralized by microbes, leading to the size-reactivity continuum model of DOM decomposition from large biopolymers into smaller, more refractory molecules. The variability in DOM removal time scales across the ocean may also relate to other ecosystem properties, such as light level or the specific metabolic capabilities of microbes in certain regions. ^{12,19,20} However, the extent to which these proposed explanations account for observed distributions of semilabile, semirefractory, and refractory DOM remains unclear.

Linking DOM composition to removal processes requires the development of molecular-level analyses that can distinguish semilabile, semirefractory, and refractory DOM fractions. The application of Fourier transform ion cyclotron resonance mass spectrometry (FT-ICR MS) to DOM characterization by direct infusion has revealed a high degree of molecular diversity based on the precise and accurate detection of thousands of molecular ion masses that can be annotated with molecular formulas. 21-30 This approach has been used to define the composition of a major component of refractory DOM as carboxylic-rich aliphatic material, which can be isolated from deep waters. 26 However, deconvolving the compositions of SLDOM and SRDOM with this approach has remained a challenge because they occur together, superimposed on a more abundant background of RDOM. Analysis of samples by direct infusion FT-ICR MS provides limited information on the spatial abundance gradients of molecular composition due to analytical issues with unresolved isomeric complexity and ion suppression. 31,32 To separate isomers and to ameliorate matrix effects that alter the sensitivity for analytes between samples, quantitative analyses typically rely on liquid chromatography coupled to mass spectrometry (LC-MS).³³ The challenge of obtaining sufficient mass precision and resolution for accurate molecular characterization and formula assignment on chromatographic time scales has recently been addressed by the development of FT-ICR MS instruments with a 21 T magnet and automatic gain control, currently the highest magnetic field available for mass spectrometry. 34-36 Mass-resolving power and spectral acquisition rates increase linearly with magnetic field strength, and the ability to collect highly accurate, well-resolved mass spectra of complex mixtures with 21T FT-ICR MS directly coupled with online liquid chromatography has been recently demonstrated. 37,38 Thus, LC-21T FT-ICR MS holds promise for resolving differences in the molecular composition of DOM fractions that have remained elusive.

The goal of this study was to decipher the molecular composition of DOM across a depth profile in the North Atlantic Gyre at the Bermuda Atlantic Time-series Study (BATS) station, where previous studies on the seasonal variability of DOC concentrations identified the accumulation of distinct DOM fractions with different removal rates. These observed DOC fractions are thought to broadly represent DOM cycling across the ocean, although concentrations and rates likely vary between ocean basins. To determine the molecular composition of DOM isolated from seawater by solid-phase extraction, we developed an open-source computational pipeline built in CoreMS for processing the data collected on an LC-ICR MS system. Scripts were developed for calibrating and attributing molecular formula assignments to LC-ICR MS data, aligning features across samples,

subtracting blanks, classifying assigned features into groups with similar spatial distributions, and evaluating chemical differences between groups. This approach was designed to be general and scalable so that it can be applied to other systems in which DOM composition is critical and poorly characterized. Our results identified molecular components of DOM that can be attributed to fractions of varying lability and provide insight into the chemical properties of DOM that underlie the persistence and turnover of this major carbon reservoir.

METHOD

Sample Collection and DOC Analysis. Samples were collected in June 2019 on the R/V Atlantic Explorer from the BATS station at 31°50′ N, 64°10′ W in the North Atlantic Ocean. Seawater samples were collected from depths spanning from 5 to 1000 m using a 24-place rosette equipped with 12 L Niskin bottles, and 10 L was transferred directly into acidcleaned high-density polyethylene carboys. Samples were then pumped through peristaltic tubing (C-flex, Masterflex) at a flow rate of 30 mL/min through poly(ether sulfone) filters (Millipore Millex-GP 0.22 μ m, 25 mm) and then into solidphase extraction (SPE) columns (1 g polystyrene divinylbenzene resin columns; ENV, Agilent). The columns were preconditioned by sequentially rinsing with 6 mL of LC-MSgrade methanol, 6 mL of ultrapure water (pH = 2; acidified with trace metal-grade HCl), and 6 mL of ultrapure water prior to sample loading. A process blank sample was prepared by priming and rinsing an SPE column without sample loading. After sample loading, the columns were rinsed with 6 mL of ultrapure water and stored frozen at -20 °C. This approach extracted approximately 10-20% of total DOC from seawater based on analyses by high-temperature combustion before and after extraction. The chemical properties of the DOM subset isolated with this approach are biased toward more hydrophobic molecules compared to bulk DOM. However, the LC-ICR MS analyses described below still enabled robust chemical properties comparisons between the depth-resolved molecular groups (corresponding to DOM components with different lifetimes) detected within this analytical window.

Immediately prior to analysis, the columns were thawed, rinsed again with 5 mL of ultrapure water, and eluted with 6 mL of methanol into polypropylene tubes. The samples were concentrated in a vacuum centrifuge to a volume below 0.5 mL until only residual water remained; then, the samples were all brought up to a final volume of 0.8 mL with ultrapure water. An internal standard of cyanocobalamin (Sigma-Aldrich BioReagent) was added to each sample (final concentration of 3 μ M), and an aliquot was transferred to reduced surface activity glass 2 mL autosampler vials (RSA, MicroSolv). Quality control samples were prepared by combining 20 μ L of each sample. This "pooled" sample was analyzed three times throughout the sample analysis batch. A comparison of the total ion chromatograms of these pooled sample analyses demonstrated reproducible retention times and sensitivity (Figure S1).

For bulk DOC measurements, seawater was collected from Niskin bottles and filtered through an inline GF/F filter, acidified with concentrated HCL to a pH of 3, and stored in precombusted borosilicate vials at room temperature. DOC concentrations were determined at the University of California, Santa Barbara by the high-temperature combustion method as described in Halewood et al.⁴⁰

LC-ICR MS Analysis. The solid-phase extracted DOM samples were analyzed by a microflow high-pressure chromatograph (UltiMate 3000 RSLCnano, Thermo Scientific) coupled to a 21 T Fourier transform ion cyclotron resonance mass spectrometer. Samples were injected in a 20 μ L volume into a microbore C18 column (0.5 \times 150 mm, 3.5 μ m particle size, Agilent Zorbax XDB-C18) held at a temperature of 30 °C. Compounds were separated using mobile phases of ultrapure water with 5 mM ammonium formate (solvent A) and methanol with 5 mM ammonium formate (solvent B). The solvent flow rate was 30 μ L/min, starting at a composition of 5% solvent B for 5 min, followed by a 30 min gradient to 95% solvent B and a 5 min hold at 95% B, before finally returning to the initial conditions. The 21 T FT-ICR MS was designed and built in the Environmental Molecular Sciences Laboratory at the Pacific Northwest National Laboratory.³⁴ The instrument was equipped with a heated electrospray ionization source set to a capillary voltage of 3200 V, sheath, auxiliary, and sweep gas flow rates of 15, 3, and 1 (arbitrary units), respectively, an ion transfer tube temperature of 300 °C, and a vaporizer temperature of 75 °C. Mass spectra were collected with a 1.5 s acquisition time with a maximum ion accumulation time of 250 ms in positive ionization mode.

To avoid batch effects, samples were analyzed out of order relative to the sampling depth. The consistency of the peak area (12% standard deviation) and retention time (13.6 \pm 0.1 min) of the extracted ion chromatogram for the cyanocobalamin internal standard (m/z=678.2918 for the doubly charged form) provided an indication of analytical stability across the analysis batch.

Data Processing. A data analysis pipeline was constructed in Python as a module of CoreMS,³⁹ a comprehensive framework for accurate high-resolution mass data analysis. Mass spectra were averaged over 2 min retention time intervals (70 spectra per interval) between 2 and 36 min above a signalto-noise ratio of 2. This signal averaging improves both the mass accuracy and the signal-to-noise ratio compared to single spectra analysis. Charge states of +1 or +2 were assigned based on the detection of ¹³C isotopologues (with a default of +1 if no isotopologues were detected). Each averaged mass spectrum was internally calibrated based on a polynomial correction applied to peaks within a siloxane and CHON series reference list that included calibrant mass peaks across the entire m/z and retention time ranges. Monoisotopic formulas were assigned to each mass peak with a search criteria that included C:1-50, H:4-100, O:1-20, N:0-4, maximum allowed double bond equivalents (DBEs) of 20, maximum H/C ratios of 3, maximum O/C ratios of 1.2, a charge state of +1, and mass error limits of ± 0.3 ppm. When multiple formulas matched a mass peak within the mass error, the formula with the highest confidence score was selected. For each monoisotopic formula assignment, all isotopologues were calculated and assigned to peaks that were less abundant than the corresponding monoisotopic peak and detected within the same mass error limit.

A combined feature list across the entire sample set was generated that contained all assigned features (molecular formulas at a specific time interval) and their intensities across the entire sample set. Features were clustered into groups based on their relative abundances across samples using *k*-means clustering with the scikit-learn machine learning Python module. Elemental ratios and the nominal oxidation state of

carbon (NOSC = 4 - [4C + H -3N - 2O]/C) were calculated for each feature based on molecular formulas.⁴²

The structural complexity of each feature was evaluated from the extracted ion chromatogram (EIC) of the corresponding m/z and retention time interval. The EICs of some features showed sharp chromatographically resolved peaks that likely correspond to a single molecular structure. These features likely represent biomolecules that are typically the targets of conventional metabolomics data processing pipelines. However, many features appeared as broad unresolved signals corresponding to complex mixtures of structural isomers, which are likely byproducts of organic matter degradation. To distinguish features representing biomolecules from polydisperse degradation products, we calculated a "dispersity index" that captured this isomeric complexity. First, the EIC of a given feature was obtained from the LC-MS data file where the feature was most abundant. The EIC data were further filtered to include the most intense points that accounted for half of the summed EIC intensity across the 2 min time interval. From this subset, the dispersity index was calculated as the standard deviation of the retention times.

Data processing scripts, core functions, and databases are available at https://github.com/boiteaulab/corems (Bermuda-Atlantic-Time-Series-Analysis-LC-21T branch). LC-ICR MS data (Thermo RAW files) are available from the Biological and Chemical Oceanography Data Management Office under Project 883936 (BCO–DMO; https://www.bco-dmo.org/project/883936). The molecular formula annotated features are available in Table S1.

RESULTS AND DISCUSSION

DOC Concentrations in the North Atlantic Gyre. Water column concentrations of DOC at the BATS station in the North Atlantic subtropical Gyre (Figure 1) exhibited well-characterized spatial and seasonal dynamics. Mixed layer DOC concentrations at BATS typically reach an annual minimum of \sim 60 μ mol kg⁻¹ during the late winter/early spring, when deep

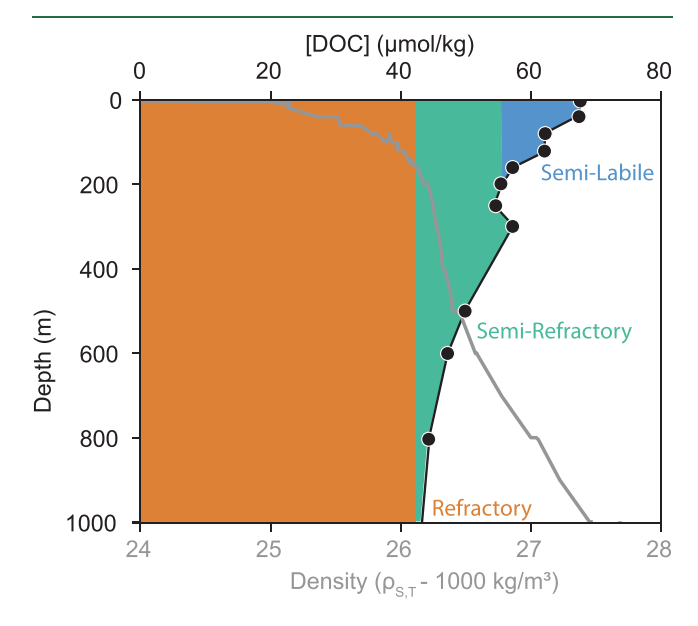


Figure 1. DOC profiles (points) and fractions (colored regions) from the Bermuda Atlantic Time-series Study site station in the North Atlantic subtropical Gyre (31°50′ N, 64°10′ W) in June 2019. The density (sigma-t) profile is shown in gray.

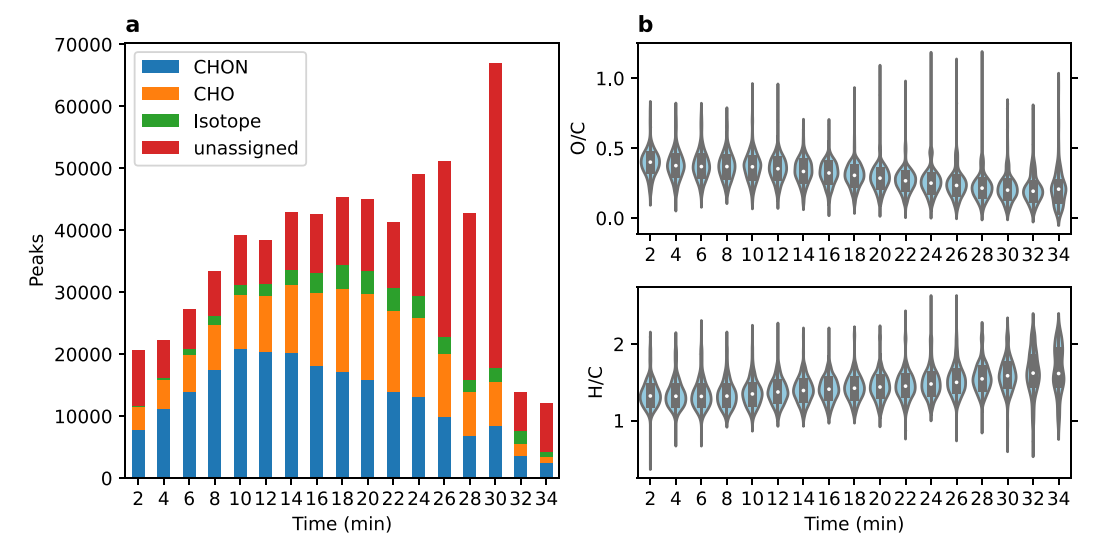


Figure 2. (a) Number of mass peaks assigned to averaged spectra within each retention time window. Colors correspond to stoichiometric chemical classes. (b) Distribution of elemental ratios of assigned mass peaks detected within each retention time window.

winter convective mixing can exceed 200 m.¹ At the time of sampling (June 2019), DOC concentrations had risen from this winter minimum, reaching 68 μ mol kg⁻¹, reflecting recent biological production and accumulation of organic matter with varying lability as the water column thermally restratifies by early summer.

Previous studies have quantified the ocean inventory and removal rate of four empirical DOC fractions that can be discerned by concentration measurements combined with water mass age tracers in biogeochemical ocean models. First, "labile" DOC is the fraction which, although accounting for a major flux of carbon through marine ecosystems, turns over within days and thus is only a minor component of the accumulated DOC pool. A second category, "semilabile" DOC, represents the majority of the DOC that accumulates in excess of the surface wintertime minimum. At BATS, annual convective mixing (Jan-March) redistributes the seasonally accumulated semilabile DOC throughout the maximal mixed layer depth, effectively exporting a portion of the surface (<100 m)-accumulated DOC into the upper mesopelagic zone (100-250 m). Subsequent restratification of the water column traps the exported DOC, where a portion is removed within the upper mesopelagic zone over months. 1,43,44 In our sampling at BATS during June 2019, semilabile DOC was observed at a concentration of 5–12 μ mol kg⁻¹ in the epipelagic zone above the mesopelagic zone maximum of 55 μ mol kg⁻¹. Within the mesopelagic zone (200-1000 m), a pool of more persistent semirefractory DOC accumulates, decaying on a time scale of decades.^{6,45} This fraction persists in excess of refractory bathypelagic DOC concentrations by approximately 4-15 μ mol kg⁻¹. Lastly, refractory DOC is defined as the fraction that is removed on a time scale of centuries to millennia and is best represented by the DOC concentrations that exist deeper than 1000 m, ⁴⁶ which range between 42 and 44 μ mol kg⁻¹ at BATS.44

Although these empirical DOC fractions capture the spatial and seasonal variability of DOC concentrations in the North Atlantic subtropical Gyre, little is known about whether (and how) the compositions of these fractions are distinct. To address this knowledge gap, we collected and analyzed solid-phase extracted DOM samples spanning the upper 1000 m

with the goal of identifying the molecular components of these spatially disparate DOM fractions.

Marine DOM Formula Assignments. We developed an automated, flexible, and scalable LC-ICR MS data processing pipeline in Python to calibrate spectra and assign molecular formulas using CoreMS. The workflow was designed to maximize the fraction of attributed peaks while implementing quality control criteria that minimized misassignments. A key advantage of 21T FT-ICR MS over other mass spectrometry platforms is its greater resolving power and mass accuracy at fast (chromatographically relevant) acquisition rates. With a 1.5 s spectral acquisition time, a resolving power $(m/\Delta m \text{ full})$ width at half-maximum) of up to 1 490 000 was obtained at m/z = 220. The resolving power decreased to 410 000 at m/z =800. Figure S2 demonstrates the extent to which a higher resolving power enables the detection of a greater number of unique chromatographic peaks. Minimum resolving powers greater than 200 000 are required to detect >90% of the peaks that were resolved by the LC-ICR MS approach in this study.

First, molecular search parameters were evaluated based on an analysis of the data from the pooled DOM sample. Initial molecular search parameters allowed molecules to have a wide range of heteroatoms $(C_{1-50}H_{4-100}O_{1-20}N_{0-8}S_{0-1}P_{0-1}Na_{0-1})$. These assignments were evaluated based on the error distributions of features containing the same heteroatom combination (e.g., CHO, CHON). However, molecular classes containing a large number of heteroatoms $(N_{5-8}S_{0-1}P_{0-1}Na_{0-1})$ had mass error distributions with significantly different means (Wilcoxon rank sum test adjusted p-value < 0.01) and distributions (Kolmogorov–Smirnov test statistic > 0.3) compared to the molecular classes with stoichiometries limited to $C_cH_hO_oN_n$ (n < 5), suggesting that some of the additional assignments obtained with the wider stoichiometric window were incorrect (Figure S3c,d). Therefore, subsequent analysis used molecular search stoichiometries of $C_{4-50}H_{4-100}O_{1-20}N_{0-4}$ as the protonated adduct. We note that this analysis was unable to distinguish ammonium adducts from molecular components with covalently associated N; thus, calculated H/C and N/C ratios were viewed as upper bounds.

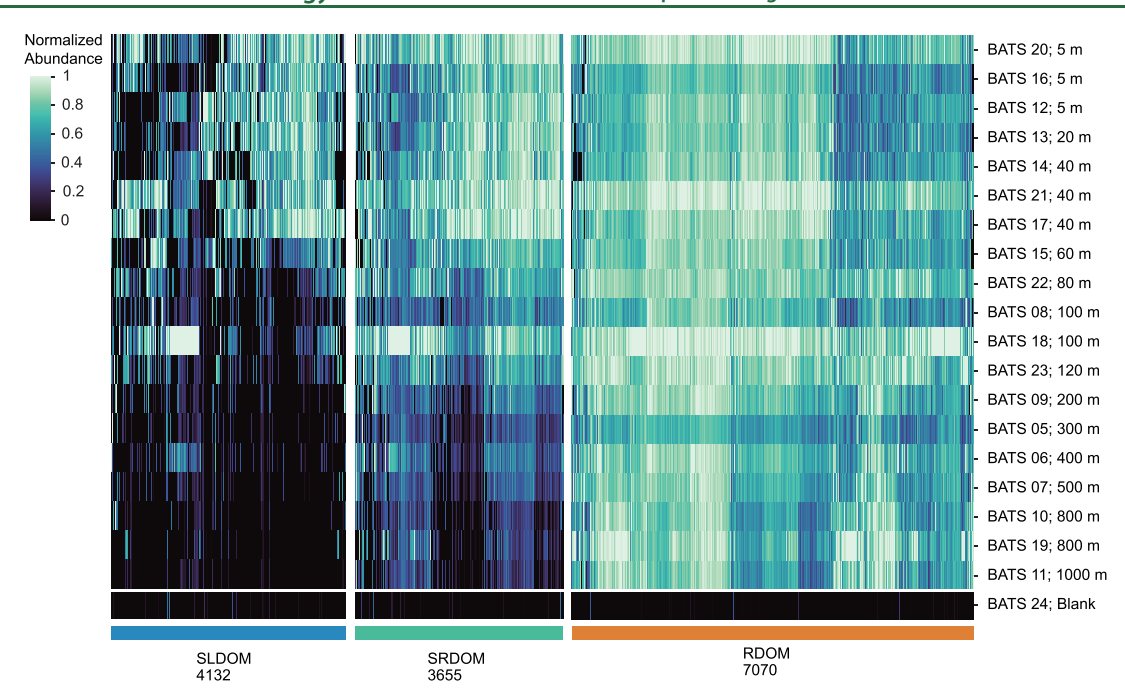


Figure 3. k-means clustering of the liquid chromatography—mass spectrometry features detected after process blank and noise filtering. Three distinct groups emerged based on similar depth distributions. Sample labels indicate analysis order and sampling depth, with the process blank shown at the bottom. The heatmap shows normalized abundances and the number of features within each group. The groups were labeled semilabile DOM (SLDOM), semirefractory DOM (SRDOM), and refractory DOM (RDOM), according to the DOC fraction that most closely resembled the depth distribution.

These search parameters were then used to assign molecular formulas to peaks detected from the marine DOM and SPE blank samples. Across all samples and retention time intervals, 63% of the averaged mass spectra peaks were assigned molecular formulas (Figure 2a). Molecular formula assignment and feature alignment yielded a list of 22 330 uniquely assigned monoisotopic features with comparable intensities throughout the water column. Features present in the SPE blank were filtered out if the maximum measured signal-to-noise ratio was <3, if the maximum intensity across all samples was less than twice the intensity observed in the blank sample, and if the feature was detected in fewer than 25% of the samples. This filtering resulted in a final list of 18 804 detected features, including 4375 unique molecular formulas (Table S1).

We evaluated the molecular stoichiometry of the assigned molecular formulas across each time bin to assess variations in molecular composition across the separation. The mean O/C ratio decreased from 0.4 to 0.21 and the mean H/C ratio increased from 1.34 to 1.67 from 2 to 34 min (Figure 2b), consistent with the expectation that more polar, oxygen-rich, condensed molecules elute at earlier retention times during a reverse phase separation. Most of the attributed formulas had O/C ratios between 0 and 0.8, H/C ratios between 1 and 2, and double bond equivalent (DBE) values of less than 16 (Figure S4).

Consistent Ion Suppression by DOM with Sample Depth. One of the main challenges of relative quantitation across samples analyzed by electrospray ionization mass spectrometry is the possibility of matrix effects that alter sensitivity, precision, and accuracy. For the analysis of marine DOM by ICR MS, the presence of thousands of co-eluted analytes within each time window raises the concern that differences in the intensity of any given feature may be attributed not to the abundance of the analyte but to

differences in the abundance of other compounds that decrease the intensity of analyte peaks by suppressing ionization. ^{33,47} While the separation of molecules by liquid chromatography reduces ion suppression relative to direct infusion analysis, there are still thousands of distinct ions that co-elute and may give rise to matrix effects.

To evaluate the extent and variability of ion suppression during the LC-ICR MS analysis of marine DOM, we compared the extracted ion chromatogram peak area of the cyanocobalamin internal standard across analyses (Figure S5). Cyanocobalamin is a suitable standard for several reasons: it is stable, has a mass outside of the range of interest in this study, and has a low background concentration in open ocean waters.⁴⁸ The mean peak area of the cyanocobalamin internal standard of the DOM samples was 32% relative to the internal standard peak area of the process blank, indicating that coeluting DOM compounds had a strong suppressive effect. Improved chromatographic separations would likely reduce the ion suppression from co-eluting molecules and enable the detection of more features. However, the variability in peak area of the internal standard across samples was low (standard deviation of 12%) and equivalent to the variability observed for analytical replicates of the pooled sample. Furthermore, there was no observed trend in the cyanocobalamin peak area with depth, even though surface DOM concentrations are higher than deep ocean DOM concentrations.

These results indicate that ion suppression was consistent across samples under the LC-ICR MS conditions in this study. This analysis provided greater confidence that variations in the intensity of features across the BATS data set could be attributed to the relative abundance rather than differences in ionization, and the outcome justified subsequent steps to interpret spatial patterns of the assigned features. Since different features may have different ionization efficiencies,

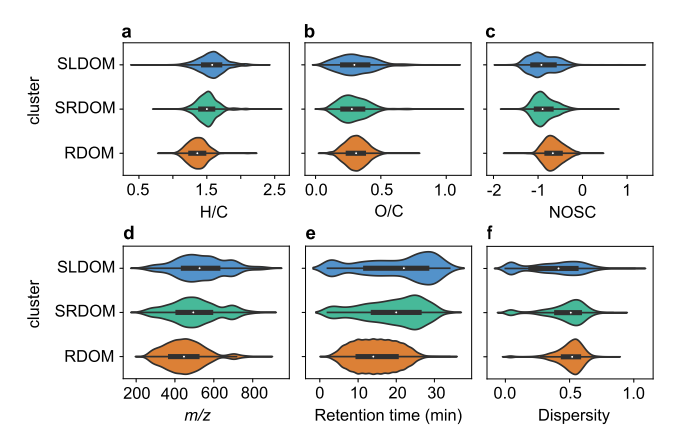
these analyses do not provide information on the absolute abundance of features without calibration with a standard of matching chemical structure.

Marine DOM Groups Based on Depth Distribution. k-means clustering was used to categorize the detected features based on the similarity of their abundances with depth (Figure 3). Clustering yielded three distinct groups of ions that exhibited strikingly similar depth distributions to the DOM lability fractions inferred from vertical gradients of the measured DOC concentrations (Figure S6).

The first group consisted of 4132 features that were most prevalent in euphotic zone samples shallower than 200 m, likely corresponding to semilabile DOM (SLDOM) produced in the euphotic zone (Figure S6a). While labile DOM was not significantly reflected in the bulk DOC measurements, such compounds were detected by LC-ICR MS as a minor component of the semilabile fraction. The second group (3655 features) had an intermediate distribution that extended throughout the water column but were, on average, 4 times more abundant at the surface compared to at 1000 m (Figures S6b), consistent with the distribution of semirefractory DOM (SRDOM) that is introduced to the mesopelagic zone by deep mixing or sinking particles. The largest group consisted of 7070 features with uniform distributions across all depths (Figure S6c). These features are likely attributed to the refractory DOM (RDOM) fraction that is uniformly distributed throughout the oceanic water column. A fourth group consisted mainly of low-abundance outlier features detected at sporadic depths (3947 features). This outlier group had similar properties to those of the RDOM group but was not considered further.

Molecular Character of Different Marine DOM Groups. We next investigated how molecular characteristics differed across the clustered groups. First, we compared the frequency distribution of molecular stoichiometric ratios, oxidation state, and molecular weights (Figure 4a-c). The H/C ratio distribution was significantly higher (indicating fewer rings and double bonds) for the SLDOM group compared to the RDOM group (mean values of 1.57 and 1.36, respectively; Wilcoxon rank-sum test p-value < 1E-100). No difference was observed for the mean O/C ratios between these groups (mean values of 0.31). The distribution of NOSC values (Figure 4c) was significantly lower (indicating less oxidized carbon) for the SLDOM group compared to the RDOM group (mean values of -0.88 and -0.65, respectively; p-value < 1E-100), resulting from the higher H/C ratio. The molecular weights (Figure 4d) of the SLDOM group were also significantly higher than those of the RDOM group (mean values of 534 and 451, respectively; p-value = 1E-90). The molecular properties of the SRDOM group were consistently in between the SLDOM and RDOM groups. Our results also show that features in the SLDOM group had later chromatographic retention times than those in the RDOM group, indicating that these molecules were generally more hydrophobic (Figure 4e). Together, these results demonstrate a general trend where more labile molecules have compositions that are more aliphatic, less oxidized, and more hydrophobic with a higher molecular weight compared to persistent molecules that occur more uniformly throughout the water

Although these molecular differences were observed for only the portion of SLDOM, SRDOM, and RDOM that was selectively extracted and detected from seawater using the



pubs.acs.org/est

Figure 4. Violin plots showing the molecular properties of LC-MS features within each DOM group defined by clustering. The (a) H/C, (b) O/C, (c) nominal oxidation state of carbon (NOSC), and (d) m/z distributions were calculated from the measured mass and assigned molecular formula of all features within each group. The (e) retention time and (f) dispersity index distributions were determined from the chromatographic characteristics of all features within each group. More hydrophobic molecules elute at later retention times, and dispersity distinguishes chromatographically resolved biomolecules (dispersity < 0.2) from unresolved complex isomeric mixtures that are likely formed from degradation (dispersity > 0.2). These results show a relationship between chemical composition and lability, where the more labile groups (SLDOM > SRDOM > RDOM) are more aliphatic, less oxidized, and more hydrophobic, have a higher molecular weight, and contain a greater proportion of resolved biomolecules compared to groups that occur more uniformly throughout the water column.

methods of this study, they mirror other observations of regional differences in marine DOM composition. Previous studies have demonstrated that the mean elemental ratios of peaks detected by direct infusion FT-ICR MS analysis of samples along the flow path of deep water appear to decrease in H/C ratio. ^{22,2.5} Bulk spectroscopic approaches have also shown trends similar to those observed by the molecular approaches presented here. Solid-state nuclear magnetic resonance (NMR) analysis of DOM isolated by reverse osmosis has indicated a greater abundance of aromatic and anomeric carbon in deep samples compared to surface samples of the North Atlantic Gyre, ⁴⁹ which is consistent with our findings of more oxidized molecules persisting in the deep ocean.

The chromatographic time dimension of the LC-ICR MS data provided additional information about the isomeric complexity of these molecular features. Figure 5 shows examples of water column profiles and extracted ion chromatograms of features from each of the three lability groups. The feature from the SLDOM group (Figure 5a) was detected as a chromatographically resolved peak at 24.8 min and exhibits an oceanographic abundance depth profile with a sharp maximum near 100 m. This feature likely represents a specific metabolite with an uncharged molecular formula of C₃₀H₅₅O₇N₁. The next profile represents a chromatographically unresolved feature within the SRDOM group with a molecular formula of C₂₉H₄₇O₇N₁. Here, the extracted ion chromatogram is broad, indicating a polydisperse mixture of isomers with the same molecular formula rather than an individual metabolite. The oceanographic distribution of this unresolved complex mixture still shows a greater abundance in the top 200 m compared to deeper samples. The final profile

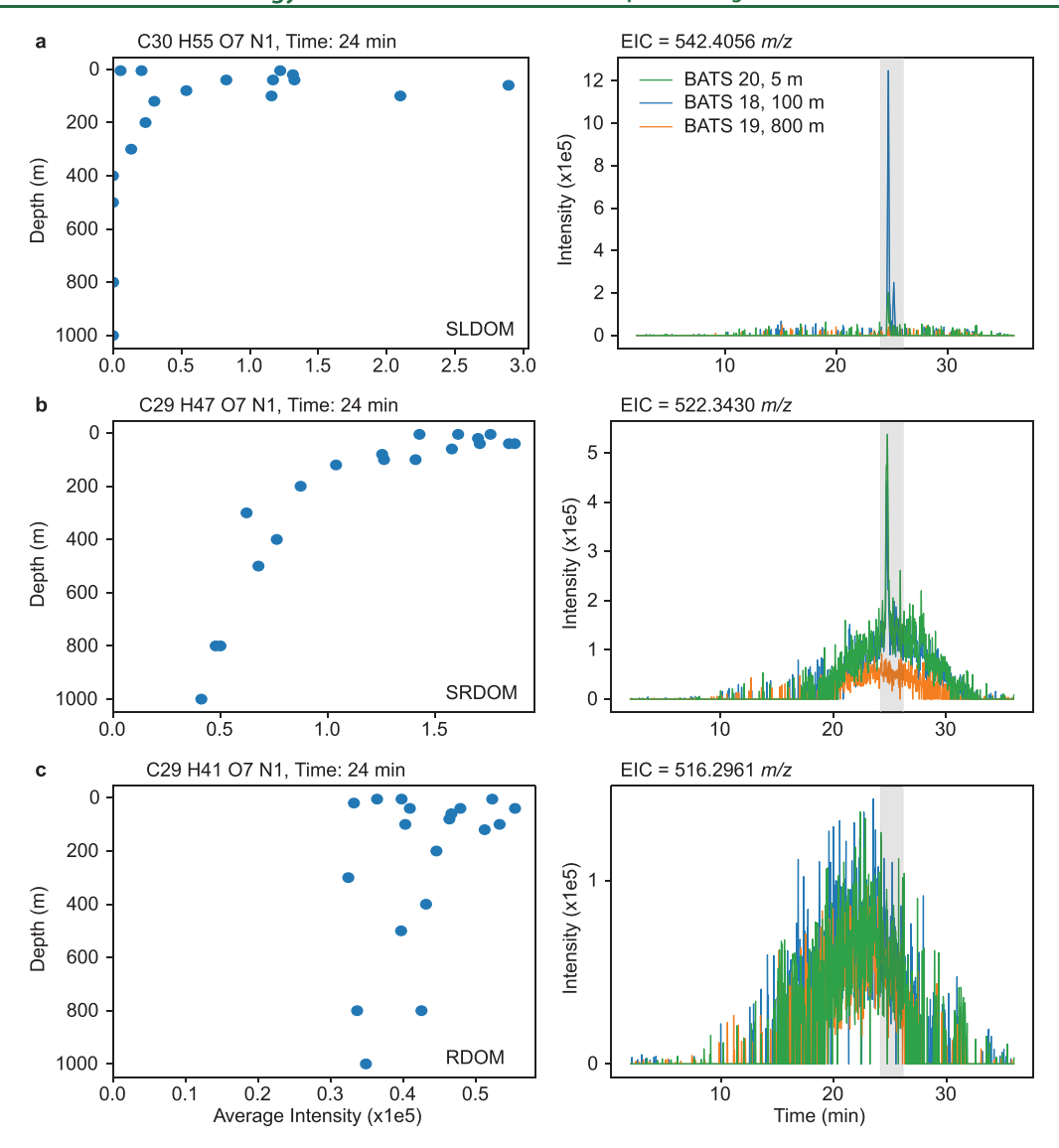


Figure 5. Examples of depth profile of features from the (a) SLDOM, (b) SRDOM, and (c) RDOM groups (left panels). Extracted ion chromatograms (EICs) of the corresponding feature protonated m/z from a representative LC-ICR MS analysis of seawater collected from 5, 100, and 800 m (right panels). Molecular formulas correspond to the uncharged molecule, and gray bars indicate the retention time interval of the feature (24–26 min).

represents another chromatographically unresolved feature that was part of the RDOM group, with a uniform distribution throughout the water column.

The extent to which molecular components of DOM represent discrete biomolecules versus isomerically complex mixtures of degradation products remains an important but open question in chemical oceanography. To distinguish these chromatographically resolved features (likely biomolecules) from unresolved complex mixtures of isomers (likely degradation products), we developed a quantitative metric of isomeric complexity based on the retention time dispersity of a feature's extracted ion chromatogram (Figure S8). Features with a dispersity index < 0.2 correspond to molecules that give rise to sharp chromatographic peaks. These structurally welldefined molecules accounted for 25%, 9%, and 2% of the features within the SLDOM, SRDOM, and RDOM groups, respectively (Figure 4f). Our analysis demonstrates that unresolved complex mixtures of degradation products dominate the composition of all lability groups and that well-resolved biomolecules that are the targets of conventional

metabolomic analyses are mostly present in the SLDOM fraction, which also likely contains labile molecules. The same chemical property trends observed in Figure 4 were preserved if the structurally well-defined features were removed from the comparison, indicating that the unresolved "degraded" components drive these distinctions between SLDOM, SRDOM, and RDOM. Our results also suggest that DOM molecular complexity (both the number of detected formulas and the number of isomeric features for each formula) decreases with depth.

The SLDOM, SRDOM, and RDOM groups also exhibited similar heteroatom class distributions, where a heteroatom class is defined as all molecular formulas with the same number of O and N atoms (Figure S9). The most common detected heteroatom classes contained 0–1 nitrogen and 4–10 oxygens across all groups. We investigated the C and H content of assignments within the three most abundant heteroatom classes. The SLDOM classes included molecules with the same basic formula of SRDOM, but they incorporated a larger number of hydrogens and, in some cases, carbons (Figure

S10). This is consistent with a view that these DOM fractions may be derived from the same biological precursor that decays into a continuum of molecules with different longevities. Previous laboratory studies have demonstrated that lipids⁵⁰ or pigments⁵¹ can undergo oxidation reactions that give rise to a chemically diverse water-soluble mixture with similar structural characteristics of marine DOM. Other studies have indicated that marine microbes grown on simple carbon substrates can generate a more complex mixture within weeks to months. ^{24,52} These experiments hint at processes that may generate polydisperse DOM in the ocean, and our results provide molecular markers that can be used to assess whether these laboratory-generated materials reflect the composition of DOM associated with specific lability fractions (Table S1).

The Fate of Marine DOM. Although LC-ICR MS only detects a narrow subset of molecules that fall within a certain molecular weight and polarity window, a comprehensive characterization of molecular stoichiometries detected within this window enables broad comparisons across groups that are likely to reflect more generalizable differences between the chemistry of more labile versus more refractory DOM fractions. Hypotheses relating DOM composition to persistence typically invoke either molecular diversity or intrinsic stability. The molecular diversity hypothesis states that DOM becomes more and more structurally diverse as it ages, which may limit microbial degradation because each component is at its minimum concentration of metabolic utility. 13,15 Our results support the notion that isomeric complexity is a characteristic of the major components of DOM that accumulate in the water column. These polydisperse components likely cycle far more slowly than structurally well-defined labile biomolecules that can be efficiently taken up and utilized by microbes, resulting in their accumulation in the water column. However, we detected isomerically complex components of SLDOM and SRDOM that did not persist below 1000 m, suggesting that the refractory DOM found in the deep ocean is not simply a more diluted and diverse mixture of molecules compared to what is found in the surface. Rather, our results demonstrate that molecular components with certain intrinsic chemical properties (smaller, less hydrophobic, and more oxidized) are more persistent in seawater.

We next investigated whether the observed differences in the molecular properties of the different DOM groups may relate to persistence based on their effects on the energetic favorability of oxidation reactions. We note that the thermodynamic stability and solubility of organic molecules are strongly dependent on specific functional groups, which were not determined in this study. Nevertheless, previous studies have found overarching correlations between the thermodynamics of oxidation and elemental stoichiometry, and this relationship has been used to estimate the energetic potential of molecules within natural organic matter. 42 Since the removal of an electron from an organic molecule becomes thermodynamically more favorable as it becomes more oxidized, the RDOM group (which has a greater NOSC value) is not expected to be inherently more resistant to oxidation compared to the more labile groups.

Instead, our results suggest that more labile molecules are more hydrophobic. This trend is demonstrated by the later chromatographic retention times of SLDOM molecules compared to RDOM molecules. Furthermore, the decrease in molecular weight and H/C ratios across the groups (SLDOM > SRDOM > RDOM) indicates a longer lifetime

for smaller molecules with a greater degree of carbon—carbon-based unsaturation and cyclization. These properties are also consistent with more labile molecules being more hydrophobic and having lower aqueous solubilities. Greater hydrophobicity may lead to faster removal via several mechanisms. More hydrophobic molecules may have enhanced removal via sorption to particles and settling out of the water column. More hydrophobic molecules with a greater propensity to form higher-molecular-weight aggregates may also be more susceptible to biodegradation, consistent with the size-reactivity continuum model of organic matter persistence. Further work is warranted to assess whether the molecular groups identified in this study exhibit differences in their reactivity with particulate phases, such as gels and minerals.

Some studies have suggested that euphotic zone processes, such as photochemical degradation or enhanced microbial activity, may be a significant sink for RDOM.^{56–58} However, the RDOM features detected by LC-ICR MS generally exhibited a similar or slightly higher abundance in the surface compared to at deeper depths. Thus, alternative mechanisms of RDOM removal, such as slow biotic or abiotic oxidation within the ocean's interior, sorption to particles, ^{46,59,60} or removal at hydrothermal vents, ⁶¹ may be more important for the component of DOM characterized in this study.

Combining the approach developed in this study with analyses that target higher-molecular-weight compounds and/ or molecules with low-abundance heteroatoms, improving the solid-phase extraction efficiency of marine DOM, and expanding the analytical window of FT-ICR MS has the potential to yield more comprehensive information about the chemical composition of DOM fractions. Previous studies have attributed high-molecular-weight DOM and neutral sugars enriched in mannose and galactose to a seasonally accumulating semilabile fraction. 62,63 These are not within the analytical window of this study, but together, they can account for >20% of surface ocean semilabile DOM. 64,65 In addition, there were unassigned mass peaks detected in the current study, which indicates the presence of molecules containing additional elements beyond C, H, O, and N. Analyses of similar seawater SPE samples using LC coupled with inductively coupled plasma mass spectrometry have demonstrated sulfur-, metal-, or halogen-containing organic species within the same analytical window. Future studies can expand the analytical window by using optimized DOM extraction methods, improving chromatographic separation, and acquiring mass spectra over narrower m/z ranges.

ASSOCIATED CONTENT

Supporting Information

The Supporting Information is available free of charge at https://pubs.acs.org/doi/10.1021/acs.est.3c08245.

Table S1: annotated feature list (XLSX)

Total ion chromatograms, resolving power required to separate DOM peaks, evaluation of molecular formula stoichiometry search parameters by mass error, data set molecular plots, internal standard detection, summed group intensity depth profiles, example of features in "outlier" DOM cluster, illustration of dispersity index calculation, heteroatom class histogram, and molecular formulas of abundant heteroatom classes (PDF)

AUTHOR INFORMATION

Corresponding Author

Rene M. Boiteau — College of Earth, Ocean, and Atmospheric Sciences, Oregon State University, Corvallis, Oregon 97330, United States; Department of Chemistry, University of Minnesota, Twin Cities, Minneapolis, Minnesota 55455, United States; Orcid.org/0000-0002-4127-4417; Email: rboiteau@umn.edu

Authors

Yuri E. Corilo – Environmental Molecular Sciences Laboratory, Pacific Northwest National Laboratory, Richland, Washington 02543, United States

William R. Kew — Environmental Molecular Sciences Laboratory, Pacific Northwest National Laboratory, Richland, Washington 02543, United States; orcid.org/ 0000-0002-4281-4630

Christian Dewey – Department of Chemistry, University of Minnesota, Twin Cities, Minneapolis, Minnesota 55455, United States; orcid.org/0000-0003-1954-8298

Maria Cristina Alvarez Rodriguez — College of Earth, Ocean, and Atmospheric Sciences, Oregon State University, Corvallis, Oregon 97330, United States

Craig A. Carlson – Department of Ecology, Evolution, and Marine Biology, Marine Science Institute, University of California, Santa Barbara, Santa Barbara, California 93106, United States

Tim M. Conway - College of Marine Science, University of South Florida, St. Petersburg, Florida 33712, United States

Complete contact information is available at: https://pubs.acs.org/10.1021/acs.est.3c08245

Author Contributions

R.M.B., T.M.C., and C.A.C. conceptualized the study and collected the samples. R.M.B. and C.A.C. analyzed the samples. R.M.B., Y.E.C., W.R.K., C.D., and M.C.A.R. contributed to the software development and data analysis. The manuscript was written through contributions of all authors. All authors have given approval to the final version of the manuscript.

Notes

The authors declare no competing financial interest.

ACKNOWLEDGMENTS

Samples were collected aboard the R/V Atlantic Explorer with the help of Ryan Schlaiss. We would like to thank Rod Johnson and the Bermuda Atlantic Time-series Study team for logistical support and Keri Opalk for the bulk DOC analyses. We acknowledge Amy McKenna for useful discussions regarding the LC-ICR MS analyses. Funding was provided by the National Science Foundation (OCE 1829761) and the Simons Foundation (Award 621513) to R.M.B., by the Simons Foundation International's BIOS-SCOPE program to C.A.C., and by the National Science Foundation (OCE 1829643) to T.M.C. This research was performed on project awards (10.46936/intm.proj.2021.60081/60000413 and 10.46936/ staf.proj.2016.49644/60006082) from the Environmental Molecular Sciences Laboratory, a DOE Office of Science User Facility sponsored by the Biological and Environmental Research program under Contract No. DE-AC05-76RL01830.

REFERENCES

- (1) Liu, S.; Longnecker, K.; Kujawinski, E. B.; Vergin, K.; Bolaños, L. M.; Giovannoni, S. J.; Parsons, R.; Opalk, K.; Halewood, E.; Hansell, D. A.; Johnson, R.; Curry, R.; Carlson, C. A. Linkages Among Dissolved Organic Matter Export, Dissolved Metabolites, and Associated Microbial Community Structure Response in the Northwestern Sargasso Sea on a Seasonal Scale. *Front. Microbiol.* **2022**, 13 (March), 1–19.
- (2) Moran, M. A.; Kujawinski, E. B.; Schroer, W. F.; Amin, S. A.; Bates, N. R.; Bertrand, E. M.; Braakman, R.; Brown, C. T.; Covert, M. W.; Doney, S. C.; Dyhrman, S. T.; Edison, A. S.; Eren, A. M.; Levine, N. M.; Li, L.; Ross, A. C.; Saito, M. A.; Santoro, A. E.; Segrè, D.; Shade, A.; Sullivan, M. B.; Vardi, A. Microbial Metabolites in the Marine Carbon Cycle. *Nat. Microbiol.* **2022**, *7* (4), 508–523.
- (3) Shen, Y.; Benner, R. Molecular Properties Are a Primary Control on the Microbial Utilization of Dissolved Organic Matter in the Ocean. *Limnol. Oceanogr.* **2020**, *65* (5), 1061–1071.
- (4) Carlson, C. A.; Hansell, D. A. DOM Sources, Sinks, Reactivity, and Budgets. In *Biogeochemistry of Marine Dissolved Organic Matter*, 2nd ed.; Elsevier, 2015; p 65–126. DOI: 10.1016/B978-0-12-405940-5.00003-0.
- (5) Hansell, D. A.; Carlson, C. A.; Schlitzer, R. Net Removal of Major Marine Dissolved Organic Carbon Fractions in the Subsurface Ocean. *Global Biogeochem. Cycles* **2012**, *26* (1), 1–9.
- (6) Hansell, D. A. Recalcitrant Dissolved Organic Carbon Fractions. *Annu. Rev. Mar. Sci.* **2013**, *5*, 421–445.
- (7) Jiao, N.; Herndl, G. J.; Hansell, D. A.; Benner, R.; Kattner, G.; Wilhelm, S. W.; Kirchman, D. L.; Weinbauer, M. G.; Luo, T.; Chen, F.; Azam, F. Microbial Production of Recalcitrant Dissolved Organic Matter: Long-Term Carbon Storage in the Global Ocean. *Nat. Rev. Microbiol.* **2010**, *8* (8), 593–599.
- (8) Moran, M. A.; Kujawinski, E. B.; Stubbins, A.; Fatland, R.; Aluwihare, L. I.; Buchan, A.; Crump, B. C.; Dorrestein, P. C.; Dyhrman, S. T.; Hess, N. J.; Howe, B.; Longnecker, K.; Medeiros, P. M.; Niggemann, J.; Obernosterer, I.; Repeta, D. J.; Waldbauer, J. R. Deciphering Ocean Carbon in a Changing World. *Proc. Natl. Acad. Sci. U. S. A.* 2016, 113 (12), 3143–3151.
- (9) Zheng, X.; Cai, R.; Yao, H.; Zhuo, X.; He, C.; Zheng, Q.; Shi, Q.; Jiao, N. Experimental Insight into the Enigmatic Persistence of Marine Refractory Dissolved Organic Matter. *Environ. Sci. Technol.* **2022**, *56*, 17420.
- (10) Ogura, N. Rate and Extent of Decomposition of Dissolved Organic Matter in Surface Seawater. *Mar. Biol.* **1972**, 13 (2), 89–93.
- (11) Ogura, N. Further Studies on Decomposition of Dissolved Organic Matter in Coastal Seawater. *Mar. Biol.* **1975**, 31 (2), 101–111.
- (12) Zakem, E. J.; Cael, B. B.; Levine, N. M. A Unified Theory for Organic Matter Accumulation. *Proc. Natl. Acad. Sci. U.S.A.* **2021**, *118* (6), No. e2016896118, DOI: 10.1073/pnas.2016896118.
- (13) Arrieta, J. M.; Mayol, E.; Hansman, R. L.; Herndl, G. J.; Dittmar, T.; Duarte, C. M. Dilution Limits Dissolved Organic Carbon Utilization in the Deep Ocean. *Science* (80-.) **2015**, 348 (6232), 331–333
- (14) Dittmar, T. Reasons Behind the Long-Term Stability of Dissolved Organic Matter. In *Biogeochemistry of Marine Dissolved Organic Matter*, 2nd ed.; Elsevier, 2015; p 369–388. DOI: 10.1016/B978-0-12-405940-5.00007-8.
- (15) Kattner, G.; Simon, M.; Koch, B. Molecular Characterization of Dissolved Organic Matter and Constraints for Prokaryotic Utilization. In *Microbial carbon pump in the ocean*; Jiao, N., Azam, F., Sanders, S., Eds.; Science/AAAS, Washington, D.C., U.S., 2011; p 60–61.
- (16) Baltar, F.; Alvarez-Salgado, X. A.; Arístegui, J.; Benner, R.; Hansell, D. A.; Herndl, G. J.; Lønborg, C. What Is Refractory Organic Matter in the Ocean? *Front. Mar. Sci.* **2021**, 8 (April), 1–7.
- (17) Kleber, M.; Bourg, I. C.; Coward, E. K.; Hansel, C. M.; Myneni, S. C. B.; Nunan, N. Dynamic Interactions at the Mineral—Organic Matter Interface. *Nat. Rev. Earth Environ.* **2021**, *2*, 402–421.
- (18) Quigg, A.; Santschi, P. H.; Burd, A.; Chin, W.-C.; Kamalanathan, M.; Xu, C.; Ziervogel, K. From Nano-Gels to Marine

- Snow: A Synthesis of Gel Formation Processes and Modeling Efforts Involved with Particle Flux in the Ocean. *Gels* **2021**, *7* (3), 114.
- (19) Carlson, C.; Giovannoni, S.; Hansell, D.; Goldberg, S.; Parsons, R.; Otero, M.; Vergin, K.; Wheeler, B. Effect of Nutrient Amendments on Bacterioplankton Production, Community Structure, and DOC Utilization in the Northwestern Sargasso Sea. *Aquat. Microb. Ecol.* **2002**, *30*, 19–36.
- (20) Letscher, R. T.; Knapp, A. N.; James, A. K.; Carlson, C. A.; Santoro, A. E.; Hansell, D. A. Microbial Community Composition and Nitrogen Availability Influence DOC Remineralization in the South Pacific Gyre. *Mar. Chem.* **2015**, *177*, 325–334.
- (21) Kujawinski, E. B.; Longnecker, K.; Blough, N. V.; Vecchio, R. D.; Finlay, L.; Kitner, J. B.; Giovannoni, S. J. Identification of Possible Source Markers in Marine Dissolved Organic Matter Using Ultrahigh Resolution Mass Spectrometry. *Geochim. Cosmochim. Acta* **2009**, 73 (15), 4384–4399.
- (22) Lechtenfeld, O. J.; Kattner, G.; Flerus, R.; McCallister, S. L.; Schmitt-Kopplin, P.; Koch, B. P. Molecular Transformation and Degradation of Refractory Dissolved Organic Matter in the Atlantic and Southern Ocean. *Geochim. Cosmochim. Acta* **2014**, *126*, 321–337.
- (23) Koch, B. P.; Ludwichowski, K. U.; Kattner, G.; Dittmar, T.; Witt, M. Advanced Characterization of Marine Dissolved Organic Matter by Combining Reversed-Phase Liquid Chromatography and FT-ICR-MS. *Mar. Chem.* **2008**, *111* (3–4), 233–241.
- (24) Koch, B. P.; Kattner, G.; Witt, M.; Passow, U. Molecular Insights into the Microbial Formation of Marine Dissolved Organic Matter: Recalcitrant or Labile? *Biogeosciences* **2014**, *11* (15), 4173–4190.
- (25) Flerus, R.; Lechtenfeld, O. J.; Koch, B. P.; McCallister, S. L.; Schmitt-Kopplin, P.; Benner, R.; Kaiser, K.; Kattner, G. A Molecular Perspective on the Ageing of Marine Dissolved Organic Matter. *Biogeosciences* **2012**, *9* (6), 1935–1955.
- (26) Hertkorn, N.; Harir, M.; Koch, B. P.; Michalke, B.; Schmitt-Kopplin, P. High-Field NMR Spectroscopy and FTICR Mass Spectrometry: Powerful Discovery Tools for the Molecular Level Characterization of Marine Dissolved Organic Matter. *Biogeosciences* **2013**, *10* (3), 1583–1624.
- (27) Kujawinski, E. B.; Del Vecchio, R.; Blough, N. V.; Klein, G. C.; Marshall, A. G. Probing Molecular-Level Transformations of Dissolved Organic Matter: Insights on Photochemical Degradation and Protozoan Modification of DOM from Electrospray Ionization Fourier Transform Ion Cyclotron Resonance Mass Spectrometry. *Mar. Chem.* **2004**, *92* (1–4), 23–37.
- (28) Kujawinski, E. B.; Longnecker, K.; Barott, K. L.; Weber, R. J. M.; Kido Soule, M. C. Microbial Community Structure Affects Marine Dissolved Organic Matter Composition. *Front. Mar. Sci.* **2016**, 3, 45.
- (29) Dittmar, T.; Koch, B.; Hertkorn, N.; Kattner, G. A Simple and Efficient Method for the Solid-Phase Extraction of Dissolved Organic Matter (SPE-DOM) from Seawater. *Limnol. Oceanogr. Methods* **2008**, 6, 230–235.
- (30) Steen, A. D.; Kusch, S.; Abdulla, H. A.; Cakić, N.; Coffinet, S.; Dittmar, T.; Fulton, J. M.; Galy, V.; Hinrichs, K.-U.; Ingalls, A. E.; Koch, B. P.; Kujawinski, E.; Liu, Z.; Osterholz, H.; Rush, D.; Seidel, M.; Sepúlveda, J.; Wakeham, S. G. Analytical and Computational Advances, Opportunities, and Challenges in Marine Organic Biogeochemistry in an Era of "Omics. Front. Mar. Sci. 2020, 7, No. 718.
- (31) Bahureksa, W.; Tfaily, M. M.; Boiteau, R. M.; Young, R. B.; Logan, M. N.; Mckenna, A. M.; Borch, T. Soil Organic Matter Characterization by Fourier Transform Ion Cyclotron Resonance Mass Spectrometry (FTICR MS): A Critical Review of Sample Preparation, Analysis, and Data Interpretation. *Environ. Sci. Technol.* **2021**, *55*, 9637–9656.
- (32) Seidel, M.; Vemulapalli, S. P. B.; Mathieu, D.; Dittmar, T. Marine Dissolved Organic Matter Shares Thousands of Molecular Formulae Yet Differs Structurally across Major Water Masses. *Environ. Sci. Technol.* **2022**, *56* (6), 3758–3769.

- (33) Trufelli, H.; Palma, P.; Famiglini, G.; Cappiello, A. An Overview of Matrix Effects in Liquid Chromatography-Mass Spectrometry. *Mass Spectrom. Rev.* **2011**, *30* (3), 491–509.
- (34) Shaw, J. B.; Lin, T. Y.; Leach, F. E.; Tolmachev, A. V.; Tolić, N.; Robinson, E. W.; Koppenaal, D. W.; Paša-Tolić, L. 21 T Fourier Transform Ion Cyclotron Resonance Mass Spectrometer Greatly Expands Mass Spectrometry Toolbox. J. Am. Soc. Mass Spectrom. 2016, 27 (12), 1929–1936.
- (35) Smith, D. F.; Podgorski, D. C.; Rodgers, R. P.; Blakney, G. T.; Hendrickson, C. L. 21 T FT-ICR Mass Spectrometer for Ultrahigh-Resolution Analysis of Complex Organic Mixtures. *Anal. Chem.* **2018**, 90 (3), 2041–2047.
- (36) Walker, L. R.; Tfaily, M. M.; Shaw, J. B.; Hess, N. J.; Paša-Tolić, L.; Koppenaal, D. W. Unambiguous Identification and Discovery of Bacterial Siderophores by Direct Injection 21 T Fourier Transform Ion Cyclotron Resonance Mass Spectrometry. *Metallomics* **2017**, 9 (1), 82–92.
- (37) Rowland, S. M.; Smith, D. F.; Blakney, G. T.; Corilo, Y. E.; Hendrickson, C. L.; Rodgers, R. P. Online Coupling of Liquid Chromatography with Fourier Transform Ion Cyclotron Resonance Mass Spectrometry at 21 T Provides Fast and Unique Insight into Crude Oil Composition. *Anal. Chem.* **2021**, *93* (41), 13749–13754.
- (38) Boiteau, R. M.; Fansler, S. J.; Farris, Y.; Shaw, J. B.; Koppenaal, D. W.; Pasa-Tolic, L.; Jansson, J. K. Siderophore Profiling of Co-Habitating Soil Bacteria by Ultra-High Resolution Mass Spectrometry. *Metallomics* **2019**, *11* (1), 166–175.
- (39) Yuri, E.; Corilo; Kew, W. R.; McCue, L. A. EMSL-Computing/CoreMS: CoreMS v1.0.0. Zenodo, 2021. DOI: 10.5281/zeno-do.4641553.
- (40) Halewood, E.; Opalk, K.; Custals, L.; Carey, M.; Hansell, D.; Carlson, C. A. Determination of dissolved organic carbon and total dissolved nitrogen in seawater using High Temperature Combustion Analysis. *Front. Mar. Sci.* **2022**, *9*, 1061646.
- (41) Buitinck, L.; Louppe, G.; Blondel, M.; Pedregosa, F.; Mueller, A.; Grisel, O.; Niculae, V.; Prettenhofer, P.; Gramfort, A.; Grobler, J.; Layton, R.; Vanderplas, J.; Joly, A.; Holt, B.; Varoquaux, G. API Design for Machine Learning Software: Experiences from the Scikit-Learn Project. *arXiv* 2013, 1.
- (42) LaRowe, D. E.; Van Cappellen, P. Degradation of Natural Organic Matter: A Thermodynamic Analysis. *Geochim. Cosmochim. Acta* 2011, 75 (8), 2030–2042.
- (43) Carlson, C. A.; Ducklow, H. W.; Michaels, A. F. Annual Flux of Dissolved Organic Carbon from the Euphotic Zone in the Northwestern Sargasso Sea. *Nature* **1994**, *371* (6496), 405–408.
- (44) Hansell, D. A.; Carlson, C. A. Biogeochemistry of Total Organic Carbon and Nitrogen in the Sargasso Sea: Control by Convective Overturn. *Deep Sea Res. Part II Top. Stud. Oceanogr.* **2001**, 48 (8–9), 1649–1667.
- (45) Carlson, C. A.; Hansell, D. A.; Nelson, N. B.; Siegel, D. A.; Smethie, W. M.; Khatiwala, S.; Meyers, M. M.; Halewood, E. Dissolved Organic Carbon Export and Subsequent Remineralization in the Mesopelagic and Bathypelagic Realms of the North Atlantic Basin. *Deep. Res. Part II Top. Stud. Oceanogr.* **2010**, *57* (16), 1433–1445.
- (46) Hansell, D. A.; Carlson, C. A. Localized Refractory Dissolved Organic Carbon Sinks in the Deep Ocean. *Global Biogeochem. Cycles* **2013**, *27* (3), 705–710.
- (47) Boysen, A. K.; Heal, K. R.; Carlson, L. T.; Ingalls, A. E. Best-Matched Internal Standard Normalization in Liquid Chromatography-Mass Spectrometry Metabolomics Applied to Environmental Samples. *Anal. Chem.* **2018**, *90* (2), 1363–1369.
- (48) Heal, K. R.; Carlson, L. T.; Devol, A. H.; Armbrust, E. V.; Moffett, J. W.; Stahl, D. A.; Ingalls, A. E. Determination of Four Forms of Vitamin B12 and Other B Vitamins in Seawater by Liquid Chromatography/Tandem Mass Spectrometry. *Rapid Commun. Mass Spectrom.* **2014**, 28 (22), 2398–2404.
- (49) Helms, J. R.; Mao, J.; Chen, H.; Perdue, E. M.; Green, N. W.; Hatcher, P. G.; Mopper, K.; Stubbins, A. Spectroscopic Characterization of Oceanic Dissolved Organic Matter Isolated by Reverse

- Osmosis Coupled with Electrodialysis. Mar. Chem. 2015, 177, 278–287.
- (50) Harvey, G. R.; Boran, D. A.; Chesal, L. A.; Tokar, J. M. The Structure of Marine Fulvic and Humic Acids. *Mar. Chem.* **1983**, *12* (2–3), 119–132.
- (51) Arakawa, N.; Aluwihare, L. I.; Simpson, A. J.; Soong, R.; Stephens, B. M.; Lane-Coplen, D. Carotenoids Are the Likely Precursor of a Significant Fraction of Marine Dissolved Organic Matter. *Sci. Adv.* **2017**, 3 (9), 1–12.
- (52) Gruber, D. F.; Simjouw, J. P.; Seitzinger, S. P.; Taghon, G. L. Dynamics and Characterization of Refractory Dissolved Organic Matter Produced by a Pure Bacterial Culture in an Experimental Predator-Prey System. *Appl. Environ. Microbiol.* **2006**, 72 (6), 4184–4191
- (53) Hertkorn, N.; Benner, R.; Frommberger, M.; Schmittkopplin, P.; Witt, M.; Kaiser, K.; Kettrup, A.; Hedges, J. Characterization of a Major Refractory Component of Marine Dissolved Organic Matter. *Geochim. Cosmochim. Acta* **2006**, *70* (12), 2990–3010.
- (54) Walker, M. A. Improvement in Aqueous Solubility Achieved via Small Molecular Changes. *Bioorg. Med. Chem. Lett.* **2017**, 27 (23), 5100–5108.
- (55) Delaney, J. S. ESOL: Estimating Aqueous Solubility Directly from Molecular Structure. *J. Chem. Inf. Comput. Sci.* **2004**, 44 (3), 1000–1005.
- (56) Mopper, K.; Zhou, X.; Kieber, R. J.; Kieber, D. J.; Sikorski, R. J.; Jones, R. D. Photochemical Degradation of Marine Organic Carbon and Its Impact on the Oceanic Carbon Cycle. *Nature* **1991**, 353 (6339), 60–62.
- (57) Stubbins, A.; Niggemann, J.; Dittmar, T. Photo-Lability of Deep Ocean Dissolved Black Carbon. *Biogeosciences* **2012**, *9* (5), 1661–1670.
- (58) Powers, L. C.; Miller, W. L. Photochemical Production of CO and CO2 in the Northern Gulf of Mexico: Estimates and Challenges for Quantifying the Impact of Photochemistry on Carbon Cycles. *Mar. Chem.* **2015**, *171*, 21–35.
- (59) Druffel, E. R. M.; Griffin, S.; Bauer, J. E.; Wolgast, D. M.; Wang, X. C. Distribution of Particulate Organic Carbon and Radiocarbon in the Water Column from the Upper Slope to the Abyssal NE Pacific Ocean. *Deep. Res. Part II Top. Stud. Oceanogr.* **1998**, 45 (4–5), 667–687
- (60) Hansell, D.; Carlson, C.; Repeta, D.; Schlitzer, R. Dissolved Organic Matter in the Ocean a Controversy Stim Ulates New Insights. *Oceanography* **2009**, 22 (4), 202–211.
- (61) Hawkes, J. A.; Rossel, P. E.; Stubbins, A.; Butterfield, D.; Connelly, D. P.; Achterberg, E. P.; Koschinsky, A.; Chavagnac, V.; Hansen, C. T.; Bach, W.; Dittmar, T. Efficient Removal of Recalcitrant Deep-Ocean Dissolved Organic Matter during Hydrothermal Circulation. *Nat. Geosci.* 2015, 8 (11), 856–860.
- (62) Goldberg, S. J.; Carlson, C. A.; Hansell, D. A.; Nelson, N. B.; Siegel, D. A. Temporal Dynamics of Dissolved Combined Neutral Sugars and the Quality of Dissolved Organic Matter in the Northwestern Sargasso Sea. *Deep. Res. Part I Oceanogr. Res. Pap.* **2009**, *56* (5), 672–685.
- (63) Goldberg, S. J.; Carlson, C. A.; Brzezinski, M.; Nelson, N. B.; Siegel, D. A. Systematic Removal of Neutral Sugars within Dissolved Organic Matter across Ocean Basins. *Geophys. Res. Lett.* **2011**, 38 (17), L17606.
- (64) Kaiser, K.; Benner, R. Biochemical Composition and Size Distribution of Organic Matter at the Pacific and Atlantic Time-Series Stations. *Mar. Chem.* **2009**, *113* (1–2), 63–77.
- (65) Kaiser, K.; Benner, R. Organic Matter Transformations in the Upper Mesopelagic Zone of the North Pacific: Chemical Composition and Linkages to Microbial Community Structure. *J. Geophys. Res. Ocean* **2012**, *117* (1), 1–12.
- (66) Boiteau, R. M.; Till, C. P.; Ruacho, A.; Bundy, R. M.; Hawco, N. J.; McKenna, A. M.; Barbeau, K. A.; Bruland, K. W.; Saito, M. A.; Repeta, D. J. Structural Characterization of Natural Nickel and Copper Binding Ligands along the US GEOTRACES Eastern Pacific Zonal Transect. Front. Mar. Sci. 2016, 3 (NOV), 1–16.

- (67) Boiteau, R. M.; Till, C. P.; Coale, T. H.; Fitzsimmons, J. N.; Bruland, K. W.; Repeta, D. J. Patterns of Iron and Siderophore Distributions across the California Current System. *Limnol. Oceanogr.* **2019**, *64* (1), 376–389.
- (68) Li, J.; Boiteau, R. M.; Babcock-Adams, L.; Acker, M.; Song, Z.; McIlvin, M. R.; Repeta, D. J. Element-Selective Targeting of Nutrient Metabolites in Environmental Samples by Inductively Coupled Plasma Mass Spectrometry and Electrospray Ionization Mass Spectrometry. Front. Mar. Sci. 2021, 8, 630494 DOI: 10.3389/fmars.2021.630494.

□ Recommended by ACS

Controls of Mineral Solubility on Adsorption-Induced Molecular Fractionation of Dissolved Organic Matter Revealed by 21 T FT-ICR MS

Zhen Hu, Mengqiang Zhu, et al.

JANUARY 24, 2024

ENVIRONMENTAL SCIENCE & TECHNOLOGY

READ 🗹

Distinct Non-conservative Behavior of Dissolved Organic Matter after Mixing Solimões/Negro and Amazon/Tapajós River Waters

Siyu Li, Norbert Hertkorn, et al.

JUNE 12, 2023

ACS ES&T WATER

READ 🗹

Characterization of a Newly Available Coastal Marine Dissolved Organic Matter Reference Material (TRM-0522)

Stacey L. Felgate, Jeffrey Hawkes, et al.

APRIL 13, 2023

ANALYTICAL CHEMISTRY

READ **C**

Dissolved Organic Matter Characteristics and Composition of Saline Lakes in the Badain Jaran Desert, China

Qiang Zhang, Junjian Wang, et al.

OCTOBER 19, 2023

ACS EARTH AND SPACE CHEMISTRY

READ 🗹

Get More Suggestions >